

Supporting Information

Luminescence Thermometry and Field Induced Slow Magnetic Relaxation based on a Near Infrared Emissive Heterometallic Complex.

Karachousos-Spiliotakopoulos, Konstantinos,^a Vassilis Tangoulis,^{a*} Nicos Panagiotou,^b Anastasios Tasiopoulos,^b Eufemio Moreno-Pineda,^c Wolfgang Wernsdorfer,^{d,e*} Michael Schulze,^e Alexandre M. P. Botas,^f Luis D. Carlos,^{f*}

- a. Department of Chemistry, Laboratory of Inorganic Chemistry, University of Patras, 26504, Patras, Greece.*
- b. Department of Chemistry, University of Cyprus, Nicosia 1678, Cyprus*
- c. Depto. de Química-Física, Escuela de Química, Facultad de Ciencias Naturales, Exactas y Tecnología, Universidad de Panamá, Panamá, Panamá.*
- d. Institute for Quantum Materials and Technology (IQMT), Karlsruhe Institute of Technology (KIT), Hermann-von-Helmholtz-Platz 1, D-76344 Eggenstein-Leopoldshafen, Germany.*
- e. Physikalisches Institut, Karlsruhe Institute of Technology, D-76131 Karlsruhe, Germany.*
- f. Phantom-g, CICECO – Aveiro Institute of Materials, Department of Physics, University of Aveiro, 3810-193 – Aveiro, Portugal*

FT-IR

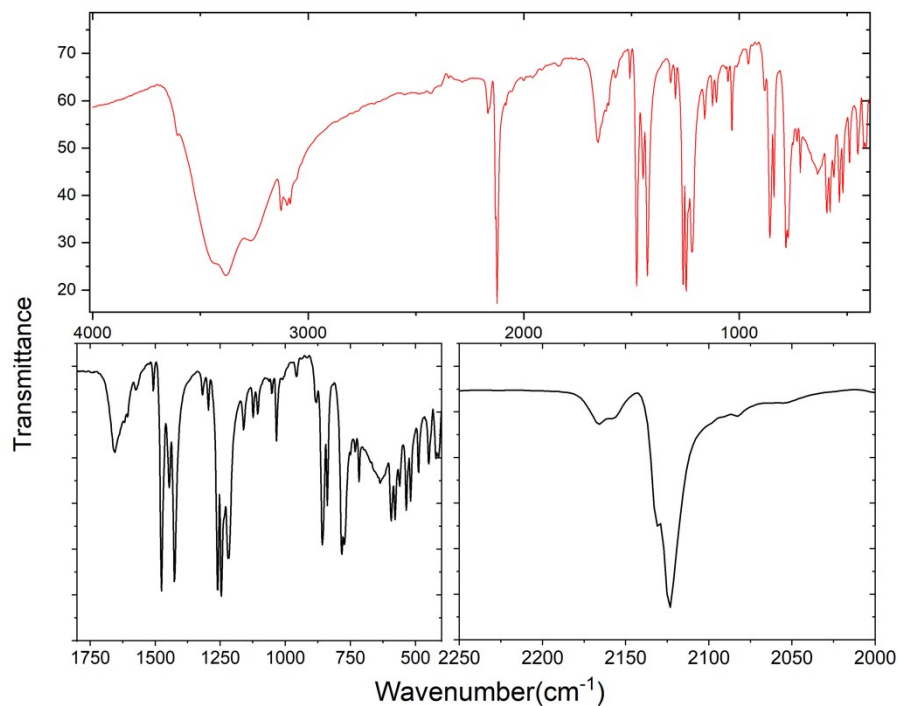


Figure S1. IR spectra of $1 \cdot 4\text{H}_2\text{O}$ in the range $4000\text{-}400\text{ cm}^{-1}$. Enlarged regions ($1600\text{-}400\text{ cm}^{-1}$ and $2200\text{-}2080\text{ cm}^{-1}$) are also presented. The bands in the $1560\text{-}1420\text{ cm}^{-1}$ region (highlighted region on the left) are assigned to the stretching vibrations of the heterocyclic rings of coordinated bpyO₂.

Crystal Packing

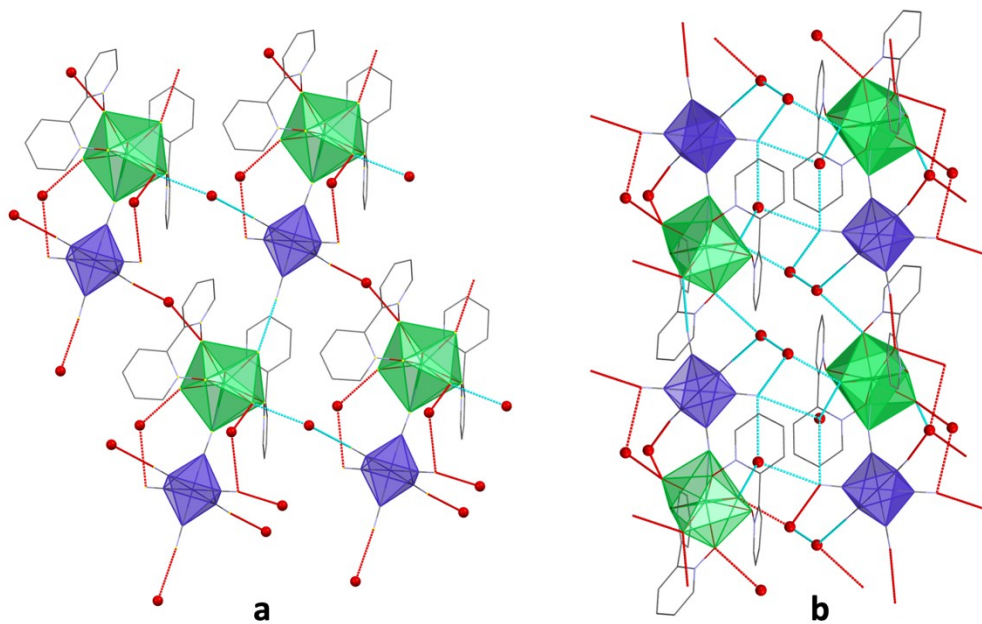


Figure S2. a) A layer of the 3D architecture of compound **1** parallel to the *ab* plane. The O-H \cdots O/N intermolecular H bonds connecting the molecules in the layer are shown in blue and red dotted lines; hanging contacts to atoms on adjacent layers are drawn with red dotted lines. c) interconnected layers through the lattice solvent H₂O molecules (oxygens are denoted as red solid spheres). The hydrogens of the solvent molecules have not been located.

Magnetic measurements

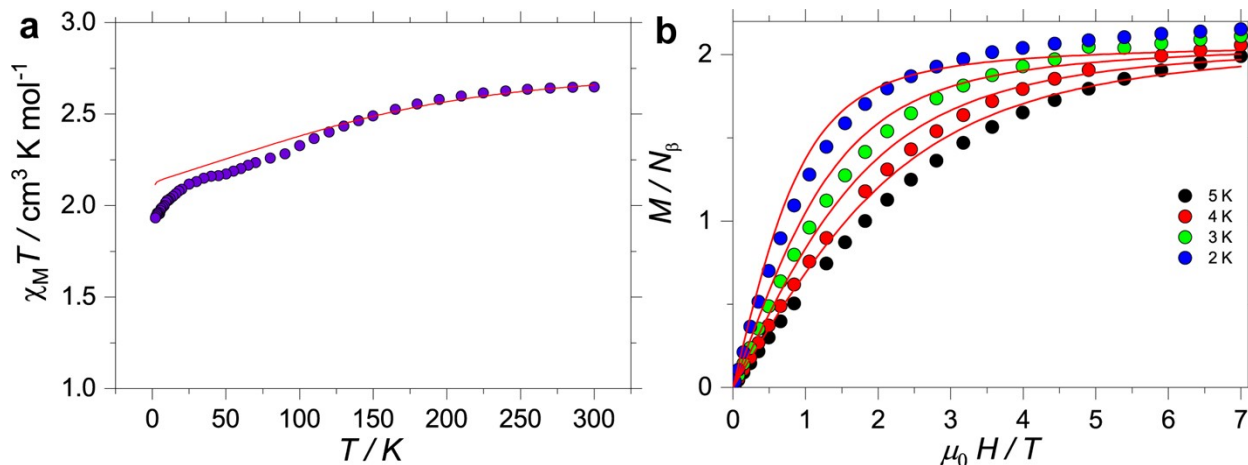


Figure S3. (a) $\chi_M T$ profile for **1** collected with $H_{DC} = 1$ kOe and (b) $M(H)$ at different temperatures. Solid lines are simulation obtained employing CASSCF results (see text for details).

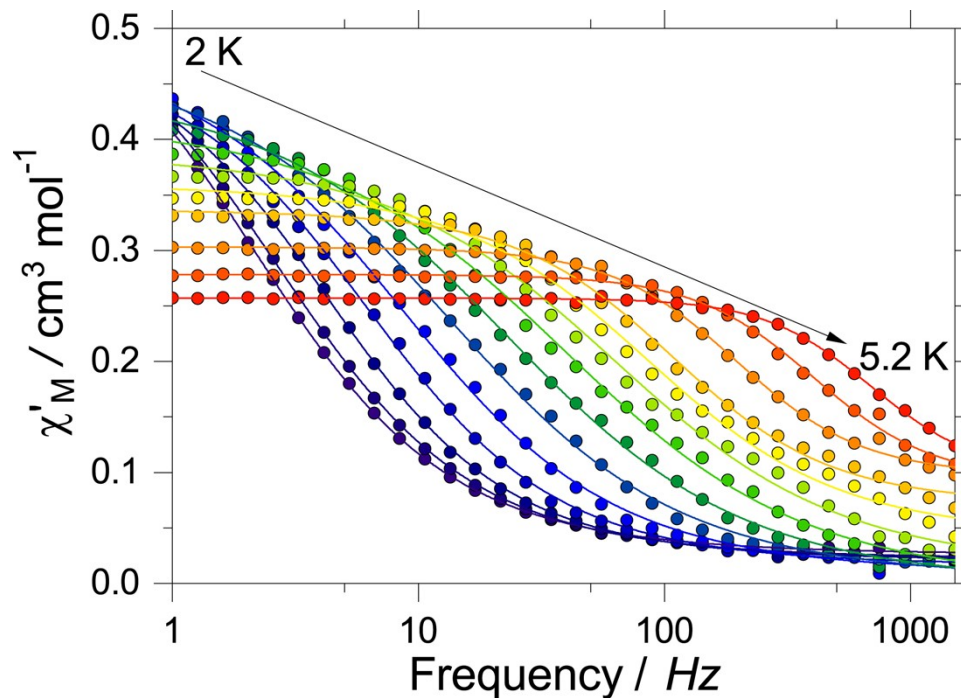


Figure S4. In-phase frequency dependent ($\chi'(\nu)$) magnetic susceptibility for **1** obtained with an oscillating field of 3.5 Oe and $H_{DC} = 1.25$ kOe in the temperature range of 2 to 5.2 K and employing frequencies between 1 to 1512 Hz.

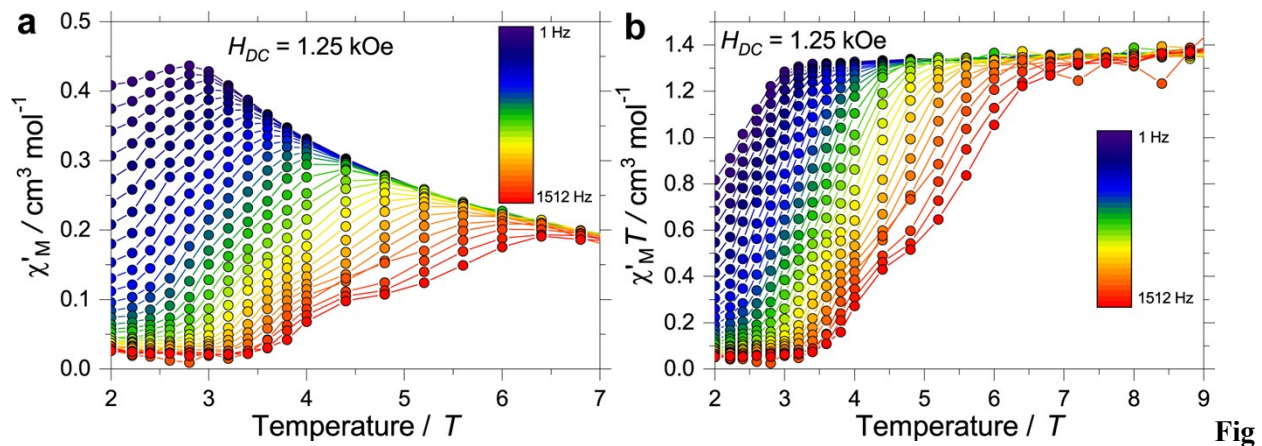


Figure S5. (a) In-phase temperature dependent ($\chi'_M(T)$) magnetic susceptibility and (b) ($\chi'_M T(T)$) for **1** obtained employing an oscillating field of 3.5 Oe and $H_{DC} = 1.25$ kOe.

Luminescence Thermometry

The relative thermal sensibility (S_r) and the temperature uncertainty (δT) are defined as:¹

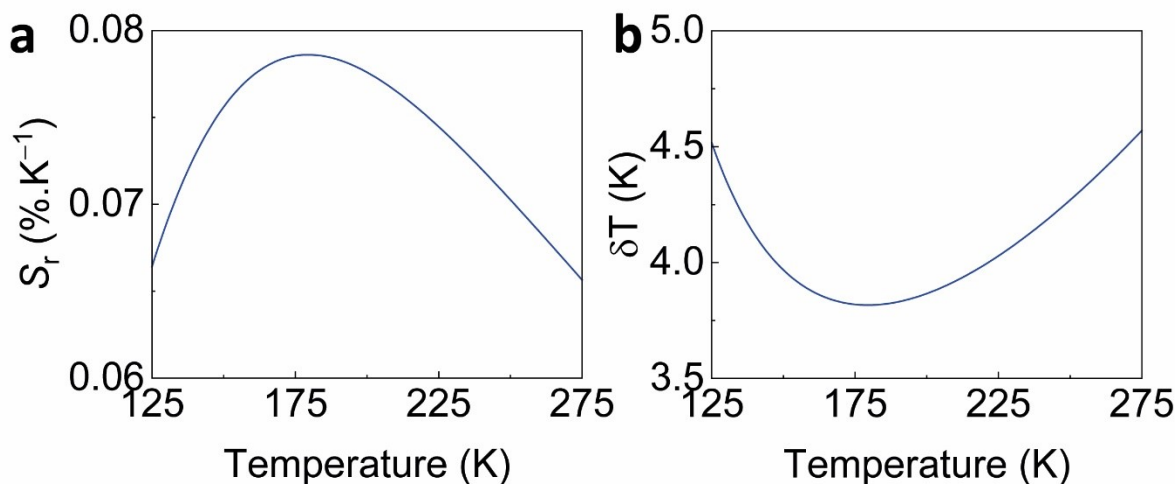
$$S_r = \frac{1}{\Delta} \left| \frac{\partial \Delta}{\partial T} \right| \quad \text{and} \quad \delta T = \frac{1}{S_r} \left| \frac{\delta \Delta}{\Delta} \right| \quad (S1)$$

where $\frac{\delta \Delta}{\Delta}$ is the relative uncertainty in Δ . The temperature uncertainty was obtained considering the experimental uncertainty associated with the thermometric parameter as:

$$(\delta \Delta)^2 = \left(\frac{\partial \Delta}{\partial I_1} \delta I_1 \right)^2 + \left(\frac{\partial \Delta}{\partial I_2} \delta I_2 \right)^2 = \Delta^2 \left[\left(\frac{\delta I_1}{I_1} \right)^2 + \left(\frac{\delta I_2}{I_2} \right)^2 \right] \quad (S3)$$

where δI_1 and δI_2 are the uncertainties in I_1 and I_2 , respectively, determined considering the standard error ($SE = 1 \times 10^5$) of the mean value of the noise signal of the spectrum (measured at

16 K in the 5882-8000 cm^{-1} range), taken $SE = \frac{\sigma}{\sqrt{N}}$, where σ is the standard derivation and



$N = 577$ is the number of points.

Figure S6. Temperature dependence of (a) S_r and (b) δT .

1. C. D. S. Brites, A. Millán, L. D. Carlos, Lanthanides in Luminescent Thermometry. In Handbook on the Physics and Chemistry of Rare Earths, Gshneidner, K. A.; Bünzli, J.-C.; Pecharsky, V., Eds. Elsevier: 2016; Vol. 48, pp 339-427.

Crystallographic Data

Table S1. Crystallographic Data for Complex **1**·4H₂O,

Empirical formula	C ₂₆ H ₁₆ CoN ₁₀ O ₁₁ Yb
Formula weight	876.46
Temperature [K]	100(2)
Wavelength [Å]	0.71073
Crystal system	Triclinic
Space group	P -1
a [Å]	10.1974(4)
b [Å]	12.2711(5)
c [Å]	13.8414(5)
a [°]	85.275(3)
b [°]	87.856(3)
c [°]	70.730(4)
Volume [Å ³]	1629.33(12)
Z	2
Density (calculated)[g/cm ³]	1.786
Absorption coefficient [mm ⁻¹]	3.434
F(000)	854
Crystal size [mm ³]	0.120 x 0.075 x 0.055
Theta range for data collection [deg]	3.326 to 27.498
Reflections collected	23274
Independent reflections	7335 [R(int) = 0.0669]
Completeness to theta = 25.242°	99.8 %
Refinement method	Full-matrix least-squares on F ²
Data / restraints / parameters	7335 / 0 / 442
Goodness-of-fit on F ²	1.055
Final R indices [I>2sigma(I)]	R _{obs} ^a = 0.0388, wR _{obs} ^b = 0.0797
R indices (all data)	R _{all} = 0.0480, wR _{all} = 0.0847
<u>Deposition Number</u>	<u>2159777</u>

$^aR = \Sigma||F_o|-|F_c|| / \Sigma|F_o|$, $wR = \{\Sigma[w(|F_o|^2 - |F_c|^2)^2] / \Sigma[w(|F_o|^4)]\}^{1/2}$ and $^bw=1/[\sigma^2(F_o^2)+(mP)^2+nP]$ where $P=(F_o^2+2F_c^2)/3$ and m and n are constants

Table S2. Selected Interatomic Distances (Å) and Angles (deg) for **1·4H₂O**,

Distance	
Yb···Co1	5.425(1)
O(1)-Yb(1)	2.346(3)
O(2)-Yb(1)	2.288(3)
O(3)-Yb(1)	2.361(3)
O(4)-Yb(1)	2.246(3)
O(5)-Yb(1)	2.325(3)
O(6)-Yb(1)	2.323(3)
O(7)-Yb(1)	2.323(3)
N(5)-Yb(1)	2.424(4)
Co1-C21	1.889(5)
Co1-C22	1.907(5)
Co1-C23	1.907(5)
Co1-C24	1.881(5)
Co1-C25	1.906(5)
Co1-C26	1.905(5)
Angle	
O1-Yb-O2	71.61(11)
O3-Yb-O4	74.27(11)
O5-Yb-O6	72.14(10)
O6-Yb-O7	144.45(11)
O2-Yb-N5	103.76(12)
O4-Yb-N5	88.92(13)
Yb-N5-C21	165.9(4)
C21-Co1-C26	177.80(19)
C22-Co1-C24	179.0(2)
C23-Co1-C25	178.3(2)
Co1-C21-N5	177.0(4)
Co1-C26-N10	178.6(4)

Table S3. Continuous Shape Measures (CShM) values for the potential coordination polyhedra of the Ln^{III} ion in the structure of complex **1**·4H₂O

CShM value ^a	Symmetry	Polyhedron
1		
32.231	<i>D</i> _{8h}	Octagon
23.167	<i>C</i> _{7v}	Heptagonal pyramid
15.012	<i>D</i> _{6h}	Hexagonal bipyramid
11.809	<i>O</i> _h	Cube
2.350	<i>D</i> _{4d}	Square antiprism
0.929	<i>D</i>_{2d}	Triangular dodecahedron
12.316	<i>D</i> _{2d}	Johnson gyrobifastigium J26
28.752	<i>D</i> _{3h}	Johnson elongated triangular bipyramid J14
2.084	<i>C</i> _{2v}	Biaugmented trigonal prism J50
1.429	<i>C</i> _{2v}	Biaugmented trigonal prism
2.941	<i>D</i> _{2d}	Snub diphenoid J84
12.622	<i>T</i> _d	Triakis tetrahedron
25.220	<i>D</i> _{3h}	Elongated trigonal bipyramid

^a The polyhedron with the smallest CShM value (in bold) is the real coordination polyhedron of the Ln^{III} center in the complex.